Dielectric Properties of the Lamellar Niobates and Titanoniobates $AM_2Nb_3O_{10}$ and $ATiNbO_5$ (A = H, K, M = Ca, Pb), and Their Condensation Products $Ca_4Nb_6O_{19}$ and $Ti_2Nb_2O_9$

Mingming Fang, Chy Hyung Kim,† and Thomas E. Mallouk*

Department of Chemistry, The Pennsylvania State University, University Park, Pennsylvania 16802, and Department of Chemistry, Chongju University, Chongju, Korea

Received November 12, 1998. Revised Manuscript Received March 31, 1999

The dielectric properties of layer perovskites in the Dion−Jacobson ($KCa_2Nb_3O_{10}$, $HCa_2Nb_3O_{10}$, $CsPb_2Nb_3O_{10}$, $HPb_2Nb_3O_{10}$, $KCa_2NaNb_4O_{13}$, $KLa_2NbTi_2O_{10}$) and Ruddlesden−Poppper ($K_2La_2Ti_3O_{10}$) series, and of related lamellar oxides ($KTiNbO_5$, $HTiNbO_5$) were measured. Most of these compounds show significant dielectric dispersion and high loss, which are attributed to both grain and grain boundary atomic displacements. The dielectric constant of $HPb_2Nb_3O_{10}$, however, is ∼150 between 1 kHz and 10 MHz, and its dielectric loss is <0.1 over the same range. Topochemical dehydration of $HTiNbO_5$ to $Ti_2Nb_2O_9$ eliminates the loss components associated with intra- and intergrain proton movement. $HCa_2Nb_3O_{10}$ undergoes a similar topochemical dehydration reaction to make a new metastable phase, $Ca_4Nb_6O_{19}$, for which a structural model is proposed. Above 550 °C, $Ca_4Nb_6O_{19}$ decomposes to a mixture of microcrystalline $CaNb_2O_6$ and $Ca_2Nb_2O_7$. Unlike $HCa_2Nb_3O_{10}$, $HPb_2Nb_3O_{10}$ does not dehydrate topochemically, but transforms directly to a mixture of $Pb_3Nb_4O_{13}$ and $PbNb_2O_6$.

Introduction

Layered inorganic compounds have been interesting to physicists, chemists, and materials scientists for many years because of their unique structures and chemical reactivity. One of their important reactions is intercalation, in which ions or molecules are included within the interlamellar galleries. Related processes are exfoliation, an extreme case of intercalation in which sheets are separated to make a colloidal suspension, and condensation, in which sheets are joined covalently to form a three-dimensional solid. Taken together these reactions provide a versatile route to many kinds of inorganic materials and thin films.

Alkali transition metal oxides represent a class of lamellar compounds that undergo all three kinds of reactions. For example, the layered compounds $ATiNbO_5$ (A = alkali metal) can be acid-exchanged and then converted to the dense titanoniobate $Ti_2Nb_2O_9$ through *chimie douce* condensation of $HTiNbO_5$. Layered perovskites in the Dion−Jacobson series,[1] such as $A[Ca_{n-1}Na_{n-3}Nb_nO_{3n+1}]$ (A = K, Rb, Cs, n = 3−7), and the Ruddlesden−Popper phases $A_2La_{n-1}Ti_nO_{3n+1}$ (A = alkali metal, n = 2−4)[2] also undergo ion exchange and intercalation, and a few cases of topochemical condensation reactions of the latter series have been reported.[3,4]

An interesting aspect of these materials is their similarity, in both composition and structure, to high dielectric and ferroelectric materials, which are often complex transition metal oxides. For example, the perovskites $BaTiO_3$, $SrTiO_3$, and $Pb(Ti_{1-x}Zr_x)O_3$ have been widely studied as ferroic materials,[5] and recent reports describe interesting new high dielectric TiO_2−Nb_2O_5−Ta_2O_5 and TiO_2−ZrO_2−SnO_2 ceramics.[6] Despite the fact that many layered perovskites have been synthesized and structurally characterized, their dielectric properties have rarely been studied. Both the dielectric properties and the condensation reactions of these lamellar materials are of interest, because the exfoliation reaction provides a potentially useful route to compound oxide films of precisely controlled thickness and composition. High dielectric oxide thin films are currently under intensive study for use in dynamic random access memories (DRAMs) and other applications.[7]

In this paper we report the frequency-dependent dielectric properties of some representative lamellar niobates and titanoniobates. Topochemical *chimie douce* reactions transform some of these materials—including layer perovskites in the Dion−Jacobson series—to three-dimensional metastable phases. Most of the alkali- and

† Chongju University.

(1) (a) Dion, M.; Ganne, M.; Tournoux, M. *Mater. Res. Bull.* **1981**, *16*, 1429. (b) Jacobson, A. J.; Johnson, J. W.; Lewandowski, J. T. *Inorg. Chem.* **1985**, *24*, 3727−3729. (c) Treacy, M. M. J.; Rice, S. B.; Jacobson, A. J.; Lewandowski, J. T. *Chem. Mater.* **1990**, *2*, 279.

(2) (a) Ruddlesden, S. N.; Popper, P. *Acta Crystallogr.* **1957**, *10*, 538; *Acta Cyst.* **1958**, *11*, 54. (b) Una, S.; Raju, A. R.; Gopalakrishnan, J. *J. Mater. Chem.* **1993**, *3*, 709.

(3) Gopalakrishnan, J.; Bhat, V. *Inorg. Chem.* **1987**, *26*, 4299.

(4) Ollivier, P. J.; Mallouk, T. E. *Chem. Mater.* **1998**, *10*, 2585.

(5) Galasso, F. S. *Structure, Properties and Preparation of Perovskite-type Compounds*; Pergamon Press: Oxford, 1969; Chapter 5.

(6) (a) Cava, R. F.; Peck, W. F., Jr.; Krajewski, J. J. *Nature* **1995**, *377*, 215−217. (b) Cava, R. F.; Peck, W. F., Jr.; Krajewski, J. J.; Roberts, G. L. *Mater. Res. Bull.* **1996**, *31*, 295−299. (c) van Dover: R. B.; Schneemeyer, L. F.; Fleming, R. M. *Nature* **1998**, *392*, 162.

(7) Kingon, A. I.; Streiffer, S. K.; Basceri, C.; Summerfelt, S. R. *MRS Bulletin*, July 1996, 46−52.

10.1021/cm981065s CCC: $18.00
Published on Web 05/06/1999

proton-exchanged lamellar compounds have relatively high dielectric loss, which is reduced somewhat by the topochemical condensation reaction, because the component that can be attributed to intragrain ionic conductivity is eliminated. Interestingly, one of the lamellar Dion−Jacobson phases ($HPbNb_2O_7$, prepared by room-temperature ion exchange of the Cs compound) has low dielectric loss and a dielectric constant of ~150 over the frequency range of 100 Hz to 10 MHz.

Experimental Section

Synthesis of Layered Perovskites and Alkali Titanoniobates. The lamellar Dion−Jacobson compound $KCa_2Nb_3O_{10}$ was prepared by grinding $CaCO_3$ (Aldrich, 99.995+%), K_2CO_3 (Aldrich, 99+%), and Nb_2O_5 (Aldrich, 99.99%) together with a ceramic mortar and pestle, and then firing the powder mixture at 1100 °C in air for 24 h.[1a] Other alkali niobates and titanates were prepared similarly. $KTiNbO_5$ was made by heating K_2CO_3, TiO_2 (anatase, Aldrich, 99.9+%), and Nb_2O_5 at 1150 °C in air for 24 h.[8] $CsPb_2Nb_3O_{10}$ was prepared by reacting Cs_2CO_3 (Aldrich, 99.9%), PbO_2 (Aldrich, 97+%), and Nb_2O_5 at 1000 °C in air for 24 h.[9] $NaNbO_3$ was prepared by heating Na_2CO_3 and Nb_2O_5 at 1000 °C in air for 24 h. $KCa_2NaNb_4O_{13}$ was prepared by heating stoichiometric amounts of $KCa_2Nb_3O_{10}$ and $NaNbO_3$ at 1200 °C in air for 48 h.[1b] $K_2La_2Ti_3O_{10}$ was prepared by heating K_2CO_3, La_2O_3, and TiO_2 at 1000 °C in air for 48 h.[2] $KLa_2NbTi_2O_{10}$ was prepared by heating K_2CO_3, La_2O_3 (Aldrich, 99.9%), Nb_2O_5, and TiO_2 at 1100 °C in air for 48 h.[10] A 20 mol % excess of K_2CO_3, Na_2CO_3, or Cs_2CO_3 was used in all these reactions to offset the volatilization of the alkali oxides at the synthesis temperature. The products were washed thoroughly with distilled water to remove excess alkali oxides, and were then dried in air. The phase purity of the products was confirmed by comparison of X-ray powder diffraction data to literature powder patterns and unit cell dimensions.

Proton exchange of the lamellar Dion−Jacobson phases and $KTiNbO_5$ was carried out at room temperature, using an excess of 4 M HNO_3. After the acid solution was stirred for 12 h, the solid was separated by filtration and exposed to a fresh solution of HNO_3. This procedure was repeated three times to ensure full exchange. The product powders were filtered, washed with water, and air-dried. Samples were digested in aqueous HF and analyzed for potassium by ICP-AES. Found (calcd) for $KCa_2Nb_3O_{10}$: 8.58 ± 0.08 (7.01). Found (calcd) for HNb_3O_{10}: 1.22 ± 0.39 (0.00).

Instrumentation and Measurements. X-ray powder diffraction patterns were obtained using a Phillips X'Pert MPD diffractometer, with monochromatized Cu Kα radiation. Thermal gravimetric analysis (TGA) and differential thermal analysis (DTA) experiments were performed on a DSC 220CU (Seiko Instruments) machine. For both measurements, the samples were heated in air at 10 °C/min.

The powders were pressed into cylindrical pellets (~1.3 cm in diameter and 1 mm thick) under a pressure of 5 tons/cm^2. Pellets of $KCa_2Nb_3O_{10}$, $KTiNbO_5$, and $CsPb_2Nb_3O_{10}$ were fired on powder beds of the same composition for 2 h at 1000 °C in air and cooled in the furnace. The pellets were then sanded smooth and coated with Au by evaporation on both sides. Variable-temperature (14−780 °C) measurements of the dielectric properties of these pressed pellets were made between 20 Hz and 1 MHz using an HP 4284 LCR Meter. Room-temperature (23 °C) measurements were made between 100 Hz and 40 MHz with an HP 4192A impedance analyzer. The resistance of the samples was measured at constant dc current (1 μA) using a Keithley 236 Source Measurement Unit.

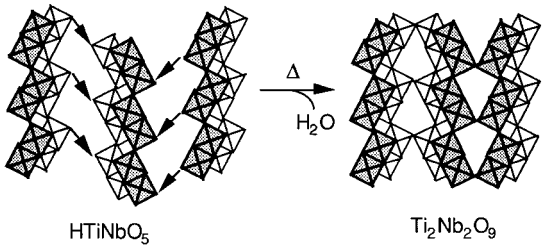

Figure 1. Schematic structural representation of the topochemical condensation of $HTiNbO_5$ to $Ti_2Nb_2O_9$, reaction 1 (data from ref 11).

Attempts to separate the ionic and electronic contributions to sample impedance were made for $KCa_2Nb_3O_{10}$ by the pulse method, using an oscilloscope (Hung Chang 5504, 40 MHz) supported by a buffering circuit designed for high resistance materials, and a pulse generator (ED Lab PG-1990). The pulse duration was 50 μs, under a constant 1 V driving voltage. However, a polarization effect due to space charge carriers with a time constant shorter than 50 μs was observed on the oscilloscope.

Results and Discussion

Dielectric Properties of Lamellar Titanoniobates and Their Topochemical Condensation Products: $KTiNbO_5$, $HTiNbO_5$, and $Ti_2Nb_2O_9$. The lamellar titanoniobate $KTiNbO_5$ can be proton exchanged to $HTiNbO_5$, and then condensed topochemically to the three-dimensional phase $Ti_2Nb_2O_9$, as described by Rebbah, et al.[11] TGA measurements confirmed that a phase transition occurs at 350 °C, with the loss of about 3.5 wt. %, corresponding to

$$2HTiNbO_5 \rightarrow H_2O + Ti_2Nb_2O_9 \qquad (1)$$

In this reaction, OH groups from adjacent layers condense, eliminating water and joining the corners of titanate and niobate octahedra, as shown schematically in Figure 1. This reaction eliminates intragrain proton motions as a possible contributor to dielectric loss, although other possible mechanisms remain.

AC impedance measurements provide quantitative information about the dielectric properties of these compounds. The dielectric constant E can be expressed as a complex function according to

$$E = k - iD \qquad (2)$$

in which the real part (k) corresponds to the in-phase component of polarization, and the out of phase part, or loss (D), is associated with the dissipation of energy.[12] The dielectric properties of $KTiNbO_5$, $HTiNbO_5$, and $Ti_2Nb_2O_9$ are summarized in Figure 2. All three compounds show substantial dispersion in the dielectric constant, and all three have high dielectric loss, especially at low frequency (<10 kHz). Suprisingly, even though $Ti_2Nb_2O_9$ has lower loss than $KTiNbO_5$ and $HTiNbO_5$, the loss is still >0.1, even at 10 MHz. These results show that interlayer cations are not the most important contributors to loss in this series of compounds, because $Ti_2Nb_2O_9$ does not contain these cations. Previous studies have shown that $HTiNbO_5$ is a

(8) Wadsley, A. D. *Acta Crystallogr.* **1964**, *17*, 623.
(9) Subramanian, M. A.; Gopalakrishnan, J.; Sleight, A. W. *Mater. Res. Bull.* **1988**, *23*, 837.
(10) Gopalakrishnan, J.; Uma, S.; Bhat, V. *Chem. Mater.* **1993**, *5*, 132.
(11) Rebbah, H.; Desgardin, G.; Raveau B. *Mater. Res. Bull.* **1979**, *24*, 1125.
(12) Brown, W. F., Jr. In *Encyclopedia of Physics*; Flugge, S., Ed.; Springer-Verlag: Berlin, 1956; Vol. 17, pp 119−123.

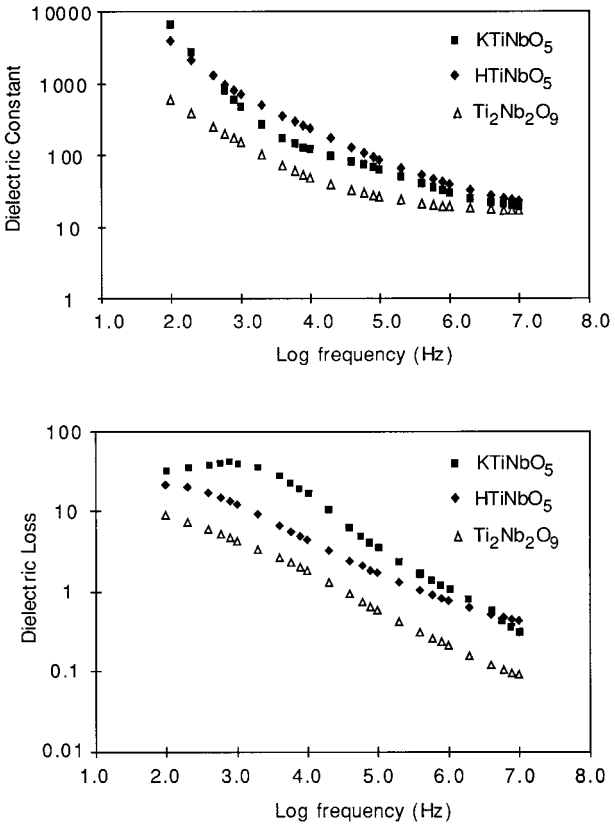

Figure 2. Dielectric constant (top) and loss (bottom) of $KTiNbO_5$ (■), $HTiNbO_5$ (◆), and $Ti_2Nb_2O_9$ (△) vs frequency at room temperature.

very poor proton conductor at room temperature ($\sigma < 10^{-8}$ ohm^{-1}cm^{-1}),[13] presumably because of the strength of interlayer O—H···O hydrogen bonding. This is consistent with the observation that the dielectric loss derives from other mechanisms, such as grain boundary ionic or segmental motion. The high loss observed with this series of compounds is rather disappointing, considering their compositional similarity to high dielectric, low loss titanoniobate ceramics.[5]

Ion-Exchange, Topochemical Condensation, and Dielectric Properties of Dion−Jacobson Phases. *A. $KCa_2Nb_3O_{10}$, $HCa_2Nb_3O_{10}$, and $Ca_4Nb_6O_{19}$.* The Dion−Jacobson phases are lamellar compounds that consist of perovskite slabs interleaved by alkali cations.[1] Their low charge density and low interlayer covalency, relative to the structurally related Ruddlesden−Popper[2] and Aurivillius[14] phases, makes them readily amenable to ion-exchange, intercalation, and exfoliation reactions.[15] Gopalakrishnan and Bhat demonstrated that the Ruddlesden−Popper phase $H_2La_2Ti_3O_{10}$ can be topochemically dehydrated to make a metastable defect perovskite.[3] We subsequently found that $H_2SrTa_{2-x}Nb_xO_7$ can be similarly dehydrated to form perovskite-type $SrTa_{2-x}Nb_xO_6$, which transforms at higher temperature to a stable tetragonal tungsten bronze form.[4] Here, we show that similar topochemical condensation reactions occur in the Dion−Jacobson series. $KCa_2Nb_3O_{10}$ was chosen as a test case, to characterize the condensation

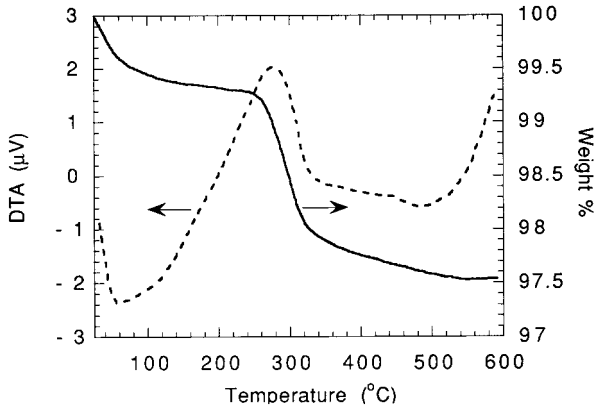

Figure 3. TGA/DTA curves showing the dehydration of $HCa_2Nb_3O_{10}$ to produce $Ca_4Nb_6O_{19}$ and the decomposition of $Ca_4Nb_6O_{19}$ to $CaNb_2O_6$ and $Ca_2Nb_2O_7$. Positive DTA signals correspond to exothermic processes.

reactions of this class of layer perovskites, and the effects of these reactions on the dielectric and transport properties.

$KCa_2Nb_3O_{10}$ can be acid-exchanged to give $HCa_2Nb_3O_{10}$, although the latter typically retains 3−5% of its potassium after a single exchange at 60 °C.[1] Our analyses show that $KCa_2Nb_3O_{10}$ contains about 1.6 wt % more K than predicted by the ideal formula, and that about the same amount (1.2 wt %) is retained in the product after three exchanges. We postulate that some of the potassium is inaccessible to ion exchange, because it is present on Ca sites in the starting material.

Jacobson and co-workers have noted that heating $HCa_2Nb_3O_{10}$ to 1000 °C results in the loss of water and formation of a mixture of stable phases, $CaNb_2O_6$ and $Ca_2Nb_2O_7$.[1] By analogy to reaction 1, one may write a condensation reaction 3, in which the metastable compound $Ca_4Nb_6O_{19}$ is formed:

$$2HCa_2Nb_3O_{10} \rightarrow H_2O + Ca_4Nb_6O_{19} \qquad (3)$$

TGA/DTA and powder X-ray diffraction data show that this compound does in fact form between about 190 and 320 °C, and decomposes above 550 °C to a mixture of $CaNb_2O_6$ and $Ca_2Nb_2O_7$. In the TGA/DTA traces (Figure 3), there is a small endothermic mass loss (0.5−0.6%) between 25 and 125 °C, which is most likely the volatilization of intercalated water.[16] This is followed by a sharp, exothermic mass loss of 1.7−1.8% (theoretical 1.73%) centered at 270 °C, corresponding to reaction 3. The disproportionation reaction 4, which begins at 550 °C, involves no change in mass, but is evident as an exotherm in the DTA trace:

$$Ca_4Nb_6O_{19} \rightarrow 2CaNb_2O_6 + Ca_2Nb_2O_7 \qquad (4)$$

The progression of X-ray powder diffraction patterns corresponding to these phase changes is shown in Figure 4. In the transition to $Ca_4Nb_6O_{19}$, the in-plane tetragonal lattice parameter (a = 3.82(2) Å) changes only slightly from that of $HCa_2Nb_3O_{10}$ (a = 3.86(1) Å). However, the layering axis, c, is compressed significantly, from 14.41(3) to 13.05(7) Å. The three-layer perovskite slabs in $Ca_4Nb_6O_{19}$ are joined with three-

(13) Rebbah, H.; Pannetier, J.; Raveau B. *J. Solid State Chem.* **1982**, *41*, 57.
(14) Aurivillius, B. *Ark. Kemi* **1949**, *1*, 463; **1950**, *2*, 519.
(15) Jacobson, A. J. *Mater. Sci. Forum* **1994**, *152−153*, 1.
(16) Jacobson, A. J.; Lewandowski, J. T.; Johnson, J. W. *J. Less Common Metals* **1986**, *116*, 137.

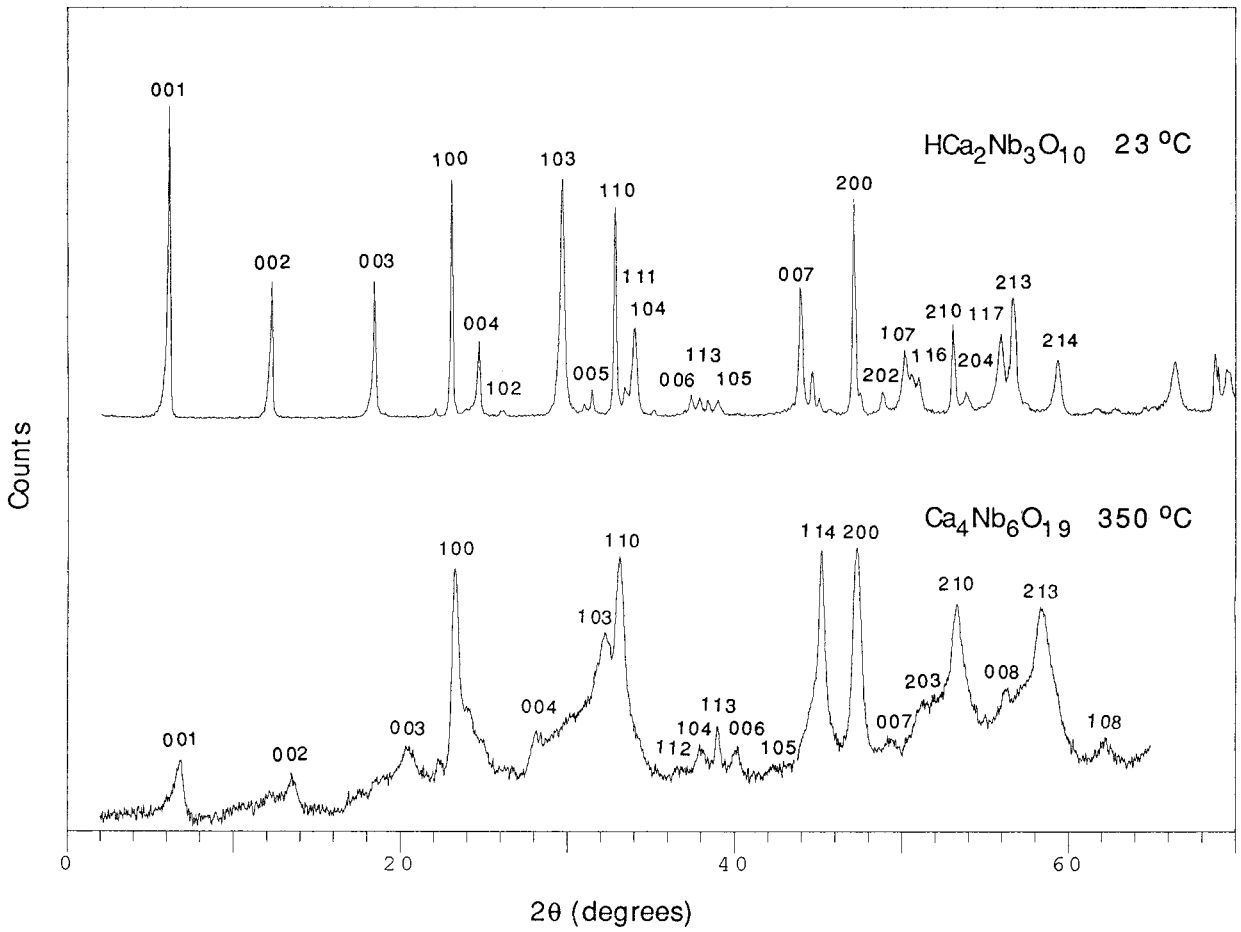

Figure 4. X-ray powder diffraction patterns of $HCa_2Nb_3O_{10}$ and $Ca_4Nb_6O_{19}$.

dimensional registry, as evidenced by the presence of $h, k, l \neq 0$ lines in the diffraction pattern. However the $00l$ layer lines are broad, indicating that the ordered domains along the stacking axis are small. Additionally, the 1.4 Å c-axis compression induced by condensation is small when one considers that a completely vertex-linked structure would have a c-axis repeat of three corner-sharing octahedra, i.e., $c \approx 3\ a = 11.5$ Å. In the second phase transition, the 13.05 Å phase disappears, and narrow lines corresponding to the structurally unrelated stable phases $CaNb_2O_6$ and $Ca_2Nb_2O_7$ appear.

These diffraction pattern of $Ca_4Nb_6O_{19}$ may be understood by recalling that layered perovskites can condense by topochemical dehydration to make three-dimensional structures.[3,4] In the case of the acid-exchanged Ruddlesden−Popper phases, such as $H_2La_2Ti_3O_{10}$, OH groups account for all the interlayer octahedral vertexes. Dehydration converts all these terminal OH groups to shared oxygen atoms. The Dion−Jacobson phases such as $HCa_2Nb_3O_{10}$, however, have only half the ion-exchange capacity of the Ruddlesden−Popper phases. In this case the interlayer octahedral vertexes consist of both OH and O groups. The former can condense to make interlayer M−O−M linkages, but the latter cannot. One possible disordered structure with the correct ratio of M−O−M and terminal M═O groups is shown in Figure 5. In $Ca_4Nb_6O_{19}$ the sheets must buckle to accommodate both groups. There is significant strain induced by juxtaposing M−O−M and M═O octahedra, so it is unlikely that these groups alternate

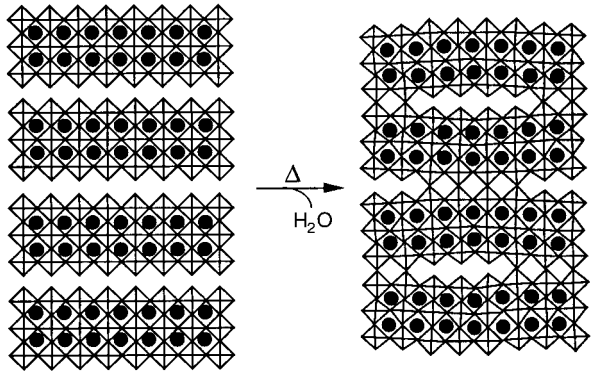

Figure 5. Structural model for the topochemical dehydration of $HCa_2Nb_3O_{10}$ to $Ca_4Nb_6O_{19}$.

in the structure. However, octahedra terminated by M═O groups are negatively charged, while the M−O−M linkages (with associated Ca^{2+} ions) are regions of local positive charge. Therefore, large domains of M−O−M or M═O are unlikely on the basis of local electroneutrality. Figure 5 represents a possible compromise between strain and electroneutrality, in which the domains of M−O−M and M═O groups are three or four octahedra wide. This model is consistent with the observed layer registry and the c-axis disorder of the metastable $Ca_4Nb_6O_{19}$ phase.

Pulse and dc conductivity measurements (Table 1) show that $HCa_2Nb_3O_{10}$ is an electronic insulator ($\sigma_{dc} < 10^{-9}$ ohm^{-1} cm^{-1}) with low proton conductivity below

Table 1. Conductivity of $HCa_2Nb_3O_{10}$ and Its Reaction Product

	conductivity (ohm^{-1} cm^{-1})					
	14 °C	130 °C	250 °C	430 °C	550 °C	670 °C
pulse method	3.0×10^{-7}	4.0×10^{-7}	1.7×10^{-7}	1.0×10^{-6}	1.4×10^{-6}	1.1×10^{-7}
dc method	insulator	insulator	insulator	6.4×10^{-7}	1.2×10^{-6}	insulator

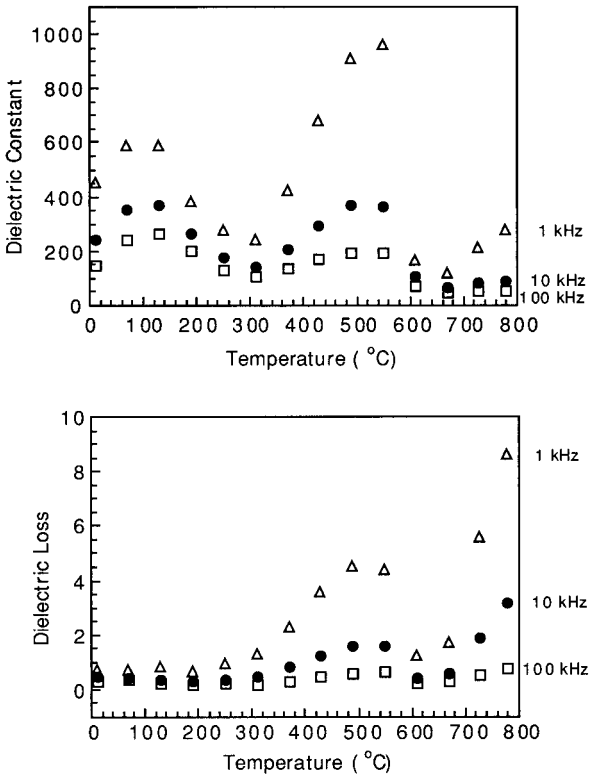

Figure 6. Dielectric constant (top) and loss (bottom) of $HCa_2Nb_3O_{10}$ at 1, 10, and 100 kHz, as it is heated and transformed first to $Ca_4Nb_6O_{19}$, and then to a mixture of $CaNb_2O_6$ and $Ca_2Nb_2O_7$.

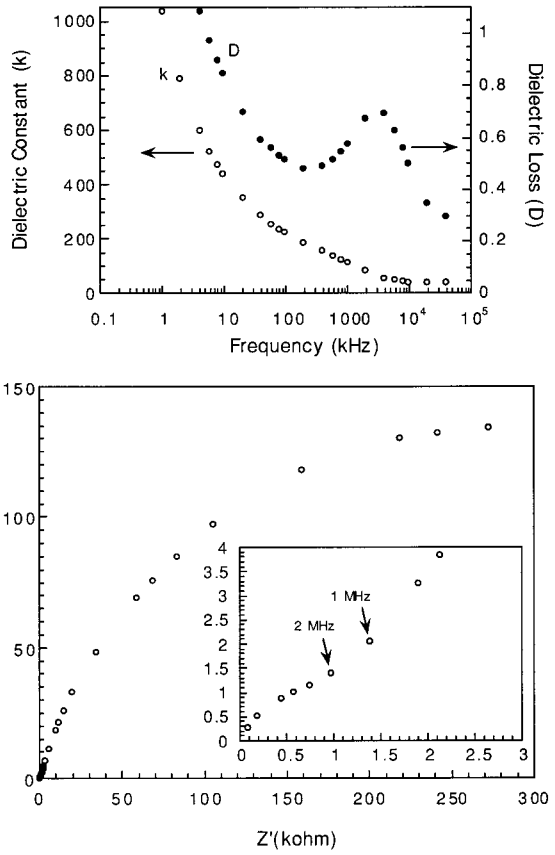

Figure 7. Frequency dependence of the dielectric constant and loss for $HCa_2Nb_3O_{10}$ at 70 °C (top), and complex impedance plot (bottom) for $HCa_2Nb_3O_{10}$. The inset plot (bottom) of $-Z''$ vs Z' at high frequency shows partial resolution of a low-impedance semicircle.

250 °C, and that the stable decomposition products, $CaNb_2O_6$ and $Ca_2Nb_2O_7$, are also electronically insulating. However, the metastable $Ca_4Nb_6O_{19}$ phase is apparently semiconducting, with a dc conductivity in the 10^{-6} ohm^{-1} cm^{-1} range. The appearance and disappearance of this semiconducting phase is reflected in the progression of changes in the dielectric constant (k) and loss (D) at 1, 10, and 100 kHz, as the Dion−Jacobson phase $HCa_2Nb_3O_{10}$ is heated through its phase transitions (Figure 6). The structural disorder that attends each first-order, exothermic phase transition is manifested as a sharp drop in k and D, which have minimum values at 300 and 670 °C. The semiconducting intermediate phase has relatively high k and D, which drop again as disproportionation to $CaNb_2O_6$ and $Ca_2Nb_2O_7$ begins occur. Both k and D then rise again as these phases are finally crystallized.

All three phases show strong dispersion in both k and D, as illustrated in Figures 6 and 7. The proton-containing phase $HCa_2Nb_3O_{10}$ additionally shows a loss peak at 3 MHz (Figure 7a), and a high frequency/low impedance arc in the complex impedance plot (inset in Figure 7b) which can be attributed to grain or grain boundary proton motion. These high-frequency features disappear in the dielectric and impedance spectra of $Ca_4Nb_6O_{19}$, and the $CaNb_2O_6/Ca_2Nb_2O_7$ phase mixture, presumably because of the absence of protons. As the $HCa_2Nb_3O_{10}$ phase is decomposed, the small arc produced by H^+ motion at high-frequency disappears and new semicircle corresponding to possible bulk relaxation begins to appear at a few hundred hertz. However, the impedance components of the higher temperature phases (bulk, grain boundary, and electrode interface) are not well resolved in their impedance plots. The impedance spectrum of $Ca_4Nb_6O_{19}$ still shows the overlap of more than two components.

Modulus spectra can be obtained by transforming the impedance data according to

$$M = k^{-1} = jwC_0Z \tag{5}$$

in which M and Z are the modulus and impedance, C_0 is the capacitance of the empty cell ($C_0 = k_0 \cdot A(\text{area})/l(\text{thickness})$, w is the angular frequency, and $k_0 = 8.854 \times 10^{-12}$ F/m). The modulus spectrum gives information about the phase isotropy, so it sometimes separates different phases even though the impedance spectrum cannot. The modulus spectra in Figure 8 appear to follow the Maxwell−Wagner model.[17] Separation of semicircles can be observed at 20−50 kHz, except for $Ca_4Nb_6O_{19}$, and the separation frequencies are different

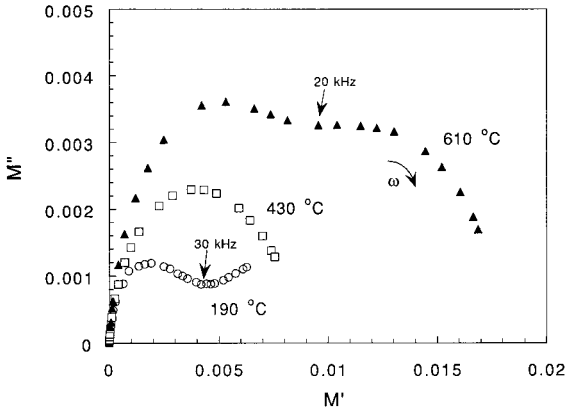

Figure 8. Modulus plots for $HCa_2Nb_3O_{10}$ at 190 °C, $Ca_4Nb_6O_{19}$ at 430 °C, and $CaNb_2O_6/Ca_2Nb_2O_7$ at 670 °C.

from those in impedance spectra. The single modulus component in the semiconducting $Ca_4Nb_6O_{19}$ phase is likely due to bulk or grain boundary segmental motion in the disordered material. The modulus spectra of the insulating $HCa_2Nb_3O_{10}$ phase, and of the insulating $CaNb_2O_6/Ca_2Nb_2O_7$ phase mixture, contain an additional high frequency semicircle that most likely arises from space charge effects at the electrode/sample interface.

B. $CsPb_2Nb_3O_{10}$ and $HPb_2Nb_3O_{10}$. Like $KCa_2Nb_3O_{10}$, the Dion−Jacobson phase $CsPb_2Nb_3O_{10}$ can be completely ion-exchanged to yield $HPb_2Nb_3O_{10}$, which is isostructural with $HCa_2Nb_3O_{10}$. Despite this similarity, the reactivity and dielectric properties of the two compounds are quite different. TGA experiments show two mass changes, occurring at 280 and 590 °C, for $HPb_2Nb_3O_{10}$. However, the X-ray powder diffraction pattern of $HPb_2Nb_3O_{10}$ is not significantly changed by heating to 350 °C, indicating the first transition is probably due to the desorption of adsorbed water. Powder patterns taken after heating to 700 °C indicate that the $HPb_2Nb_3O_{10}$ is decomposed in the second transition to a mixture of $Pb_3Nb_4O_{13}$ and $PbNb_2O_6$, according to

$$2HPb_2Nb_3O_{10} \rightarrow H_2O + Pb_3Nb_4O_{13} + PbNb_2O_6 \quad (6)$$

The mass change in the 590 °C transition is only 0.6%, which is significantly less than that expected for reaction 6 (1.05%). It appears that much of the water loss occurs gradually, prior to the reaction that produces microcrystalline $Pb_3Nb_4O_{13}$ and $PbNb_2O_6$ phases.

The dielectric properties of $CsPb_2Nb_3O_{10}$ and $HPb_2Nb_3O_{10}$ are summarized in Figure 9. While $CsPb_2Nb_3O_{10}$ shows significant dispersion in its dielectric constant and loss curves, the dielectric constant of $HPb_2Nb_3O_{10}$ is ~150 over a wide frequency range (1 kHz to 10 MHz), and the loss is <0.1 over the same range.

C. $KLa_2NbTi_2O_{10}$, $K_2La_2Ti_3O_{10}$, and $KCa_2NaNb_4O_{13}$. Several variations in A and B site cations are possible within the Dion−Jacobson and Ruddlesden−Popper series. To survey the effect of substituting Ti for Nb and of increasing the layer charge density, three other layer perovskites were prepared and their dielectric properties were also measured. X-ray powder diffraction patterns

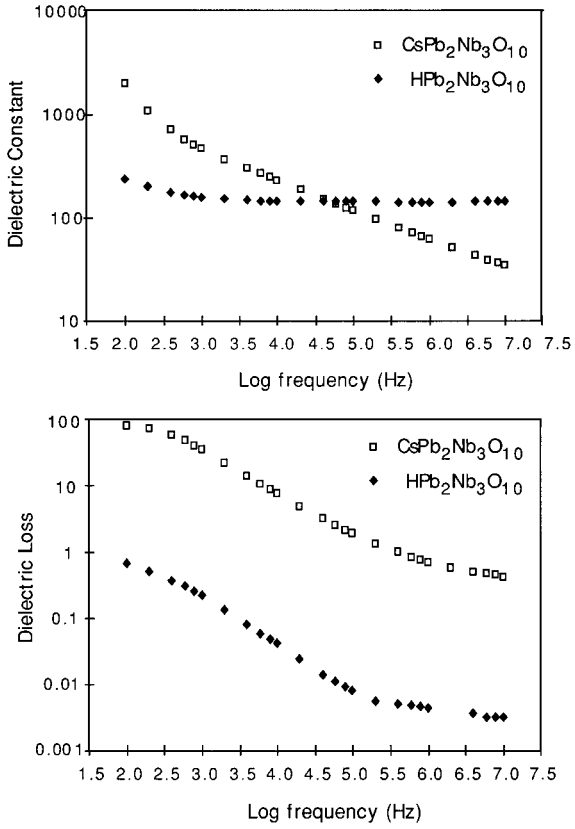

Figure 9. Dielectric constant (top) and loss (bottom) vs frequency for $CsPb_2Nb_3O_{10}$ and $HPb_2Nb_3O_{10}$.

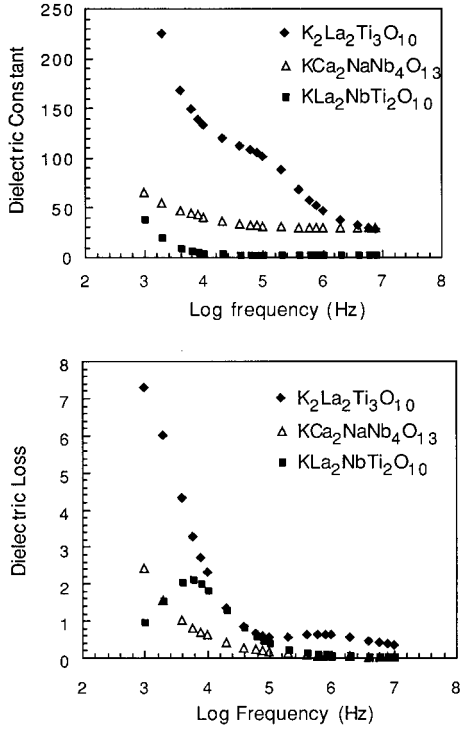

Figure 10. Dielectric constant (top) and loss (bottom) vs frequency for the Ruddlesden−Popper compound $K_2La_2Ti_3O_{10}$, and for Dion−Jacobson compounds $KCa_2NaNb_4O_{13}$ and $KLa_2NbTi_2O_{10}$.

of these compounds were in close agreement with literature reports, and showed that they were single-phase materials. Figure 10 shows the dielectric properties of these compounds. All three compounds show

(17) MacDonald, J. R. *Impedance Spectroscopy*; Wiley-Interscience: New York 1987; p 200.

significant dispersion in the dielectric constant and have relatively high dielectric loss at low frequency.

Conclusions

The topochemical condensation reactions of $HTiNbO_5$ and $HCa_2Nb_3O_{10}$ result in the formation of the metastable three-dimensional solids $Ti_2Nb_2O_9$ and $Ca_4Nb_4O_{19}$. The latter is the first example of such a condensation reaction in the Dion−Jacobson family of layered perovskites.

While elimination of interlayer OH groups causes a modest decrease in the dielectric loss, both materials have substantial loss, which arises from bulk segmental and/or intergrain atomic displacement. The reasons for the very low dielectric loss of the Dion−Jacobson compound $HPb_2Nb_3O_{10}$, relative to several other structurally similar materials, is not clear. The ionic conductivity of $HPb_2Nb_3O_{10}$ (8×10^{-6} ohm^{-1} cm^{-1}) is quite similar to that of $CsPb_2Nb_3O_{10}$ (6×10^{-6} ohm^{-1} cm^{-1}) at 500 K. Dion et al. measured the ionic conductivity of a series of $MCa_2Nb_3O_{10}$ (M = Rb, Tl, Cs, K) compounds and found that $KCa_2Nb_3O_{10}$ has $\sigma_{500K} = 1 \times 10^{-9}$ ohm^{-1} cm^{-1}, which is much smaller than that of $HPb_2Nb_3O_{10}$.[1] Bulk ionic conductivity is therefore not well correlated with dielectric loss for layered perovskites. It is possible that intergrain ionic conductivity, or space-charge effects of the gold−oxide interface, are responsible for the higher dielectric losses of $KCa_2Nb_3O_{10}$, $HCa_2Nb_3O_{10}$, $KTiNbO_5$, and $HTiNbO_5$. Temperature-dependent complex impedance measurements are currently underway to elucidate the dielectric properties of this family of layered materials, as are measurements of the dielectric properties of the thin films derived from them.[18]

Acknowledgment. This work was supported by the National Science Foundation (CHE-9529202) and the Defense Advanced Research Projects Agency.

CM981065S

(18) Fang, M.; Kim, H.-N.; Saupe, G. B.; Kim, H.-N.; Waraksa, C. C.; Miwa, T.; Fujishima, A.; Mallouk, T. E. *Chem. Mater.* **1999**, *11*, 1526 (following article in this issue).